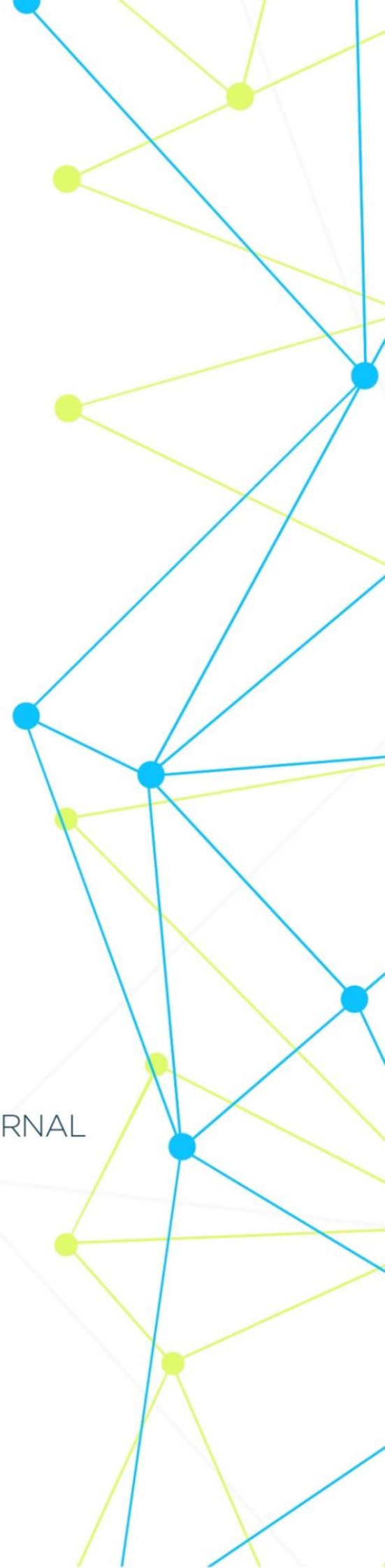


INTERNATIONAL MEDICAL SCIENTIFIC JOURNAL

# **ART OF MEDICINE**



Founder and Publisher **North American Academic Publishing Platforms**

**Internet address:** <http://artofmedicineimsj.us>

**E-mail:** [info@artofmedicineimsj.us](mailto:info@artofmedicineimsj.us)

**11931 Barlow Pl Philadelphia, PA 19116, USA +1 (929) 266-0862**

## **CHIEF EDITOR**

**Dr. Pascual Izquierdo-Egea**

## **EDITORIAL BOARD**

**Prof. Dr. Francesco Albano**

**Prof. Dr. Tamam Bakchoul**

**Dr. Catherine J. Andersen**

**Prof. Dr. Pierre-Gregoire Guinot**

**Prof. Dr. Sandro Ardizzone**

**Prof. Dr. Rainer Haak**

**Dr. Dmitriy Atochin**

**Prof. Henner Hanssen**

**Prof. Dr. Antonio Aversa**

**Available at** <https://www.bookwire.com/>

**ISBN:** [978-0-578-26510-0](https://www.isbn-international.org/product/9780578265100)

### Ways to optimize the therapy of coronavirus infection caused by COVID -19.

Abilov P.M., Iriskulov B.U., Saydalikhodjaeva O.Z., Boboeva Z.N., Azimova S.B., Usmonova G.E.

For corresponding author: [pulatabilov1985@mail.ru](mailto:pulatabilov1985@mail.ru)

Abilov Pulat Melisovich - assistant, basic doctoral student of the Department of Normal and Pathological Physiology of TMA, e-mail: [pulatabilov1985@mail.ru](mailto:pulatabilov1985@mail.ru)

Iriskulov B.U. - DSc, Professor, Head of the Department of Normal and Pathological Physiology of TMA, e-mail: [iriskulov.tma@mail.ru](mailto:iriskulov.tma@mail.ru)

Saydalikhodjaeva Ozoda Zamanovna – PhD, Associate professor of the Department of Normal and Pathological Physiology of TMA, e-mail: [ozoda.tma@mail.ru](mailto:ozoda.tma@mail.ru)

Boboeva Zuhra Nurillaevna – PhD, senior lecture of the Department of Normal and Pathological Physiology of TMA, e-mail: [zuhra.tma.uz](mailto:zuhra.tma.uz)

Azimova Sevara Bakhodirovna – DSc, assistant of the department of Normal and Pathological Physiology of TMA, e-m

Usmonova Gulchekhira Erkinovna – PhD, assistant of the Department of Normal and Pathological Physiology of TMA, e-mail: [gulchekhira.tma@mail.ru](mailto:gulchekhira.tma@mail.ru)

**Abstract.** After electrophoresis, the results of 7 separate PCR reactions for each SARS-CoV-2 strain were converted into a binary matrix for subsequent in silico analysis. Positive amplification results were recorded as “1”, and negative ones as “0”, indicating the presence or absence of a specific DFR locus in a particular representative of SARS-CoV-2. Thus, the treatment of coronavirus infection with a new combination drug based on G. Lucidum and black cumin is a pathogenetically substantiated method.

Primers with a high content of G+C form a stronger bond with the template, which means that their ability to bind to partially non-complementary DNA regions increases. This should lead to the amplification of a larger number of fragments and an increase in the differentiating ability of the RAPD method. Thus, the detection and elimination of coronavirus infection caused by SARS CoV-2 is achieved after the use of a new drug based on G. Lucidum and black cumin (95% CI = 1.3-5.6 at  $\chi^2 = 0.9321007$ , U (Mann- Winnie) = 0.8721093, H (Kruskes-Wallis test) = 0.9102385 at  $p \leq 0.05$

**Keywords:** SARS CoV-2; G. Lucidum; Alkhadaya; CD4+; CD8+; polymerase chain reaction

**Introduction.** Immune patterns of COVID-19 include lymphopenia, lymphocyte activation and dysfunction, granulocyte and monocyte abnormalities, increased cytokine production, and elevated antibodies. Lymphopenia is a key feature in patients with COVID-19, especially in severe cases. CD69, CD38, and CD44 are highly expressed on patients' CD4+ and CD8+ T cells, and virus-specific T cells in severe cases show a central memory phenotype with high levels of IFN- $\gamma$ , TNF- $\alpha$ , and IL-2. However, lymphocytes exhibit a depletion phenotype with activation of programmed cell death protein-1 (PD1), immunoglobulin T-cell domain and mucin domain-3 (TIM3), and lectin-like killer cell receptor subfamily C member 1 (NKG2A) [3]. The level of neutrophils is significantly higher in severe patients, while the percentage of eosinophils, basophils and monocytes is reduced. Increased production of cytokines, especially IL-1 $\beta$ , IL-6 and IL-10, is another key characteristic of severe COVID-19. IgG levels are also elevated and there is a higher total antibody titer [8].

Since the discovery of the new SARS-CoV-2 coronavirus, scientists have been arguing about its origin [6]. It has been suggested that SARS-CoV-2 is the product of laboratory manipulation. However, genetic data do not support this hypothesis and show that SARS-CoV-2 did not originate from a previously known viral backbone [9].

coronavirus genomes show that SARS-CoV-2 has unique features that distinguish it from other coronaviruses: optimal affinity for the angiotensin -converting enzyme 2 (ACE2) receptor and a polybasic cleavage site at the junction of the S1/S2 spikes, which defines infectivity and host range [7,10].

SARS-CoV-2 is very similar to bat SARS-like coronaviruses [2], and bats may be a reservoir host. RaGT13 is approximately 96% identical to SARS-CoV-2, with some differences in the spike

receptor binding domain (RBD), which may explain differences in ACE2 affinity between SARS-CoV-2 and SARS-like coronaviruses .

The SARS-CoV-2 multibase cleavage site is absent from the pangolin beta coronavirus , which shares similarities with SARS-CoV-2. In addition, the RBD sequence of the spike protein (S) indicates that it arose as a result of a natural evolutionary process [1].

Estimates of the most recent common ancestor of SARS-CoV-2 date the epidemic to between late November 2019 and early December 2019, which is consistent with the first reported cases. Thus, after the zoonotic event and before the acquisition of the polybasic furin cleavage site , undetected transmission to humans occurred.

There is also a growing focus on another natural product known as the G mushroom . *Lucidum* . The composition of this natural product is very wide, including superoxide dismutase , which also reduces the pathogenetic effect of the “ cytokine storm” without causing side effects on the liver .

Also recently, more and more attention has been paid to another natural product *Alhadaya* , which is black cumin oil. I noticed that and *G . Lucidum* and *Alhadaya* contain carboxyl groups in their composition, and they are not a continuation of nitro groups and sulfhydryl groups. These carboxyl groups extend from the G phenolic rings . *Lucidum* and *Alkhaday* 's benzene rings , and the idea of creating a new drug based on *G* was proposed . *Lucidum* and *Alkhaday*, and given the importance not only in the treatment of coronavirus infection, but also in its safe use, then this study is considered a hot topic and requires further study.

**The aim of the study.** To evaluate the impact of a new vector therapy ( *G. lucidum* , *Alkhadaya* ) for SARS - CoV - 2 coronavirus infection .

**Materials and research methods.** To achieve this goal, the results of treatment of 50 patients with coronavirus infection caused by COVID -19 were analyzed . All patients were divided into groups: group 1 - patients with coronavirus infection with a confirmed positive PCR test, treated with ivermectin at a dosage of 300 mg body weight ( n = 15), group 2 - patients with coronavirus infection treated with baicalin at a dose of 500 mg ( n = 15), group 3 - patients with coronavirus infection treated with molnupiravir 25 mg/kg body weight ( n = 15), 4 group - patients with coronavirus infection treated with a new drug based on *G . Lucidum* and *Alhadaya* ( n =15).

SARS - CoV -2 strains in the mycelial growth phase were cultivated on agar Sabouraud ( Difco , USA) at 28°C for 30 days. Cultural and morphological studies of cultures of strains were carried out in accordance with generally accepted requirements.

SARS - CoV - 2 culture grown in the mycelial phase was suspended in a 0.15 M NaCl solution , filtered through a gauze filter and disinfected by adding sodium merthiolate solution to a final concentration of 0.1 mg/ml, followed by heating for 40 min at 56±1° C and incubation at room temperature for 24 h.

For RAPD typing of *H. capsulatum* collection strains , the following primers were used : 1281 (5'-AACGCGCAAC-3'), 1283 (5'-GCGATCCCCA-3'), 1253 (5'-GTTTCCCGCCC-3') [ Kersulyte D. et al ., 1992]. Primers were synthesized by CJSC Sintol (Moscow). DNA amplification using "hot start" was carried out in a volume of 25 µl . The reaction mixture contained: 10 - 20 ng of genomic DNA of the studied *H. capsulatum* strain , 15 pmol of each of the oligonucleotide primers for a two primer reaction or 20 pmol for a single primer reaction, 200 µM of each deoxyribonucleoside triphosphate and 10 µl of blue-2 PCR buffer containing Taq polymerase. To prevent evaporation, 30 µl of mineral oil was layered on the surface of the mixture . Amplification was carried out on a thermal cycler " Tertsik " (NPF "DNK-technology", Moscow) in the following mode: preheating 94 °C - 5 min, 45 cycles (94 °C - 30 s, 35 °C - 30 s, 72 °C - 60 s), final elongation 72 °C – 5 min.

Statistical processing was carried out taking into account parametric and nonparametric research methods.

**Research results** . The results of panel testing before treatment are shown in Table 1.

**Table 1. Results of testing a panel of PCR samples.**

Sample	SARS-CoV-2	COVID-19
--------	------------	----------

1 group (positive)	+	+
group 2 (positive_	-	+
group 3 (positive)	+	+
4 group (positive)	+	+

After electrophoresis, the results of 7 separate PCR reactions for each SARS - CoV -2 strain were converted into a binary matrix for subsequent analysis in silico . Positive amplification results were recorded as “1”, and negative ones as “0”, which indicated the presence or absence of a specific DFR locus in a particular representative of SARS - CoV -2. The obtained DFR profiles of collection strains were supplemented with profiles of SARS - CoV -2 strains obtained as a result of analysis in silico nucleotide sequences from the Broad database Institute of MIT and Harvard .

After treatment in group 1 (treatment with ivermectin), the results of PCR tests are shown in Table 2.

**Table 2. Results of treatment with ivermetin (group 1) using PCR test.**

Pool size	SARS-CoV-2	COVID-19
6 plasma samples	-	-
6 plasma samples	+	+
6 plasma samples	-	+
6 plasma samples	+	+

Table 3 shows the results of treatment with baicalin (group 2) using a PCR test.

**Table 3. Results of treatment with baicalin (group 2) using a PCR test.**

Pool size	SARS-CoV-2	COVID-19
6 plasma samples	+	+
6 plasma samples	-	+
6 plasma samples	+	-
6 plasma samples	-	+

Table 4 shows the results of treatment with molnupiravir (group 3) using a PCR test.

**Table 4. Results of treatment with molnupiravir (group 3) using PCR test.**

Pool size	SARS-CoV-2	COVID-19
6 plasma samples	+	-
6 plasma samples	-	-
6 plasma samples	+	+
6 plasma samples	-	-

Table 5 presents the treatment results of the new combination drug based on G . Lucidum and Alkhadai .

**Table 5 Treatment outcomes of the new combination drug based on G . Lucidum and Alhadaya .**

Pool size	SARS-CoV-2	COVID-19
6 plasma samples	-	-
6 plasma samples	-	-
6 plasma samples	-	-
6 plasma samples	+	-

Thus, the treatment of coronavirus infection with a new combination drug based on G. Lucidum and Alhadaya is a pathogenetically substantiated method.

Primers with a high content of G+C form a stronger bond with the template, which means that their ability to bind to partially non- complementary DNA regions increases. This should lead to the

amplification of a larger number of fragments and an increase in the differentiating ability of the RAPD method.

Thus, when carrying out amplification reactions with arbitrary primers 1253, 1281, and 1283 differing in GC composition, stable, reproducible, specific sets of RAPD spectra of collection strains of *H. capsulatum* were obtained. The highest resolution of intraspecific typing was found in PCR with primer 1283.

Figure 1 shows an example of a dendrogram of electrophoretic RAPD profiles of SARS - CoV -2 strains based on primer 1283. With a genetic distance coefficient of 0.25, SARS - CoV -2 strains were divided into 8 groups: Group I - T-3-1, 6652, 12/89, 6651 (100% homology), 6650 and DO-2; T-4;10-X; Group II - C-15; III group - 28, 23 and 510; IV group - 638, B-580; Group V - 630; group VI - J-185-B, J-185-P (100% homology); Group VII - 73004, 1 and 73002; Group VIII - B-681, BM-87 (100% homology).

**Rice. 1. Genotyping SARS - CoV -2 and its dendrogram.**

	2	3	4	4	7	8	9	0	0	0	1	2	4	4	5	5	6	8	8	9	9	0	1	6	6	7	7	8	9	2	3	5	7	8	8	9	9	
Hcc 1	C	A	T	G	A	T	C	A	A	C	G	C	T	A	A	A	A	-	-	C	C	A	G	C	G	C	A	A	A	A	G	A	C	T	G	C	G	
Hcc 22	.	.	.	.	.	G	-	-	-	A	T	G	.	C	T	T	-	A	A	.	G	T	.	G	.	.	.	.	.	.	.	.	.	.	.	.	.	.
Hcc 23	.	.	.	.	.	G	-	-	-	A	T	G	.	C	T	T	-	A	A	.	S	G	T	.	G	.	.	.	.	.	.	.	.	.	.	.	.	.
Hcc 28	.	.	.	.	.	G	-	-	-	A	T	G	.	C	T	T	-	A	A	.	G	T	.	G	.	.	.	.	.	.	.	.	.	.	.	.	.	.
Hcc 510	.	.	.	.	.	G	-	-	-	A	T	G	.	C	T	.	-	A	A	.	G	T	.	G	.	.	.	.	.	.	.	.	.	.	.	.	.	.
Hcc 6650	.	.	.	.	.	G	-	-	-	A	T	G	.	C	T	.	-	A	A	.	G	T	.	G	.	.	.	.	.	.	.	.	.	.	.	.	.	R
Hcc 6651	.	.	.	.	.	G	-	-	-	A	T	G	C	C	T	.	A	A	A	.	G	T	.	G	.	.	.	T	T	.	.	.	.	.	.	.	.	
Hcc 6652	.	.	.	.	.	G	-	-	-	A	T	G	C	C	T	.	A	A	A	.	G	T	.	G	.	.	.	.	W	.	G	.	.	.	.	.	.	
Hcc 73002	.	.	.	.	.	A	.	.	.	.	T	.	.	.	.	-	A	.	.	G	.	.	.	.	.	.	.	.	.	.	.	.	.	.	.	.	.	.
Hcc 73004	.	.	.	.	.	G	.	.	.	A	T	G	.	.	G	.	-	A	.	.	C	.	.	.	.	.	.	.	.	.	.	.	.	.	.	.	.	.
Hcc B-580	.	.	.	.	.	G	-	-	-	A	T	G	.	C	T	.	A	A	A	.	G	T	.	G	.	.	.	.	.	.	.	.	.	.	.	.	.	.
Hcc C-15	.	.	.	.	.	G	-	-	-	A	T	G	.	C	T	.	A	A	A	.	G	T	.	G	.	.	.	.	.	.	.	.	.	.	.	.	.	.
Hcc DO-2-T	.	.	.	.	.	G	-	-	-	A	T	G	.	C	T	T	-	A	A	.	G	T	.	G	.	.	.	.	.	.	.	.	.	.	.	.	.	.
Hcc J-185-B	.	.	W	R	.	.	.	.	.	.	.	.	.	.	.	.	.	.	.	.	.	.	.	.	.	.	.	.	.	.	.	.	.	.	.	.	.	.
Hcc J-185-P	.	.	.	.	.	.	.	.	.	.	.	.	.	.	.	.	.	.	.	.	.	.	.	.	.	.	.	.	.	.	.	.	.	.	.	.	.	.
Hcc T-3-1	.	.	.	.	.	G	-	-	-	A	T	G	.	C	T	T	-	A	A	.	G	T	.	G	.	.	.	.	.	.	.	.	.	.	.	.	.	.
Hcd 630	.	W	.	.	G	.	.	.	.	C	.	.	T	.	.	.	-	A	.	G	.	G	.	G	.	.	.	.	.	.	.	.	.	.	.	R	Y	
Hcd B-638	.	.	.	.	G	.	.	.	.	C	.	.	T	.	.	.	.	-	A	.	G	.	G	.	G	.	W	.	.	.	.	.	.	.	.	.	.	
Hcd B-681	.	.	.	.	G	.	.	.	.	C	.	.	T	.	.	.	T	-	A	.	G	.	G	.	G	.	.	.	.	.	.	.	.	.	.	T	.	.
Hcd BM-87	.	.	.	.	G	.	.	.	.	C	.	.	T	.	.	.	T	-	A	.	G	.	G	.	G	.	.	.	.	.	.	.	.	.	.	.	.	
Hcf 1289	T	.	.	.	.	G	-	-	-	A	T	G	C	C	T	.	A	A	A	.	G	T	.	T	G	.	T	T	.	.	.	.	.	.	.	.	.	

Analysis of electrophoretic RAPD profiles showed that all strains of SARS - CoV - 2, regardless of the primers used, had a similarity coefficient < 40 %, which indicates a high degree of heterogeneity of the studied strains. Depending on the primers and strains, 12-21 DNA fragments were registered, the size of which ranged from 114 to 1206 bp. When comparing the RAPD profiles of 20 strains of the causative agent of histoplasmosis, only one common species-specific amplicon obtained by carrying out the amplification reaction with a combination of primers 1283 and 1253.

Thus, all used paired combinations of oligonucleotide primers had a higher differentiating ability compared to a single primer. As a result of our cluster analysis of RAPD patterns obtained using one and a combination of two primers, groups of SARS - CoV -2 strains were formed, the number and composition of which varied depending on the primers.

**Conclusion** \_ Typing of SARS - CoV - 2 based on phenotypic traits is limited due to their relatively low variability. In this regard, to date, none of the phenotypic markers provides the necessary efficiency in deciphering outbreaks of coronavirus infection. Therefore, genetic typing methods come to the fore in the study of the intraspecific diversity of the COVID -19 pathogen. Summarizing the literature data, we can conclude that the search for the optimal genotyping scheme for SARS - CoV -2 strains is still ongoing. Moreover, at present, there is no generally accepted methodological approach to the differentiation of strains of the COVID -19 pathogen, as well as an established set of genetic markers. Based on the foregoing, the relevance of scientific research

aimed at studying the polymorphism of the genomes of SARS - CoV -2 strains and the selection of optimal markers for genetic typing of the SARS - CoV -2 pathogen is obvious.

Serological and molecular methods to identify infectious markers are not alternative, they complement each other.

Detection methods are direct methods in which virus genomes are directly determined. These methods allow detecting the presence of infection in the early stages, having high sensitivity and specificity. However, in the chronic course of the disease, the concentration of viral nucleic acids in the blood may be lower than the sensitivity of the reagent kits used. In this case, a negative test result for the presence of coronavirus infection will be obtained . In this situation, the use of methods that detect protein targets will determine the presence of the disease. Viral protein products are present in the blood of infected individuals longer than viral nucleic acids. Antiviral antibodies synthesized by cells of the immune system in response to a viral infection appear several weeks after infection and can persist throughout life at detectable concentrations.

Thus, the detection and destruction of the coronavirus infection caused by SARS CoV -2 is achieved after the application of a new drug based on G . Lucidum and Alhadaya (95% CI = 1.3-5.6 at  $\chi^2 = 0.9321007$ , U (Mann-Winney test) = 0.8721093, H (Kruskes- Wallis test) = 0.9102385 at  $p \leq 0.05$

**Conclusions.** The analysis of the effect of a new combination drug based on G . Lucidum and Alhadaya showed that the inclusion of this drug is pathogenetically justified and has a high significance.

The study of a strain of coronavirus infection according to the PCR method is the most predictable according to the study.

**References:**

1. An experimental assessment of the influence of Ganoderma Lucidum on the state of oxidative stress / Iriskulov BU, Saydalikhodjaeva OZ, Abilov PM, Seytkarimova GS, Norboeva SA, Musaev Kh.A. \_ // International journal of scientific & technology research, Volume 9, Issue 03, March 2020: 6645-6649
2. Aromatic constituents from Ganoderma lucidum and their neuroprotective and antiinflammatory activities / Shuang -Yang Li et at. // Fitoterapia , <https://doi.org/10.1016/j.fitote.2019.01.013>
3. Bioactive metabolites of Ganoderma Lucidum : Factors, mechanism and broad spectrum therapeutic potential / Chetan Sharma et at. // Journal of Herbal Medicine, <https://doi.org/10.1016/j.hermed.2019.10.002>
4. Characterization, hypolipidemic and antioxidant activities of degraded polysaccharides from Ganoderma Lucidum / Yu Xu et at. // International Journal of Biological Macromolecules, <https://doi.org/10.1016/j.ijbiomac.2019.05.166>
5. Clinical and functional evaluation of the effectiveness of treatment of chronic catarrhal gingivitis in children with the use of biologically active additives based on Ganoderma Lucidum // Abilov PM, Makhkamova FT / Pediatric, Scientific and practical journal, No. 1, 2018: 108-111
6. Comparison on characterization and antioxidant activity of polysaccharides from Ganoderma lucidum by ultrasound and conventional extraction / Qiaozhen Kang et at. // International Journal of Biological Macromolecules, <https://doi.org/10.1016/j.ijbiomac.2018.11.215>
7. Dayaolingzhiols AE, AchE inhibitory meroterpenoids from Ganoderma lucidum / Qi Luo et at. // Tetrahedron, <https://doi.org/10.1016/j.tet.2019.04.022>
8. Development of Ganoderma lucidum spore powder based proteoglycan and its application in hyperglycemic, antitumor and antioxidant function / Li-Fang Zhu et at. // Process Biochemistry, <https://doi.org/10.1016/j.procbio.2019.05.025>
9. DNA damaging potential of Ganoderma lucidum extracts / Maria Soledad Vela Gurovic et at. // Journal of Ethnopharmacology , <https://doi.org/10.1016/j.jep.2018.02.005>
10. Efficiency of individual prophylaxis of dental caries using dental gel Ispring based on Ganoderma Lucidum in schoolchildren in Tashkent // Abilov PM / Journal Dental and Oral Health 5: 1-4, 2018